Electron properties of fluorinated single-layer graphene transistors

F. Withers,[1] M. Dubois,[2] and A. K. Savchenko[1]
[1]*Centre for Graphene Science, School of Physics, University of Exeter, Exeter EX4 4QL, United Kingdom*
[2]*Laboratoire des Matériaux Inorganiques, Clermont Université–UBP, CNRS-UMR 6002, 63177 Aubière, France*
(Received 2 June 2010; revised manuscript received 18 July 2010; published 6 August 2010)

We have fabricated transistor structures using fluorinated single-layer graphene flakes and studied their electronic properties at different temperatures. Compared with pristine graphene, fluorinated graphene has a very large and strongly temperature-dependent resistance in the electroneutrality region. We show that fluorination creates a mobility gap in graphene's spectrum where electron transport takes place via localized electron states.

DOI: 10.1103/PhysRevB.82.073403 PACS number(s): 72.80.Vp, 73.22.Pr

Graphene, a gapless semiconductor with "massless" charge carriers, is a material with many unusual electron properties and potential for new device applications.[1] However, in a graphene-based transistor the absence of the gap in the band-structure results in a relatively small resistance difference between the electroneutrality (Dirac) region and a region with large carrier concentration (i.e., between the "on" and "off" states). This can become a significant limitation in its use in electronics and intensive research is currently underway aimed at the creation of a (tunable) gap in graphene's energy spectrum. One direction is functionalization of graphene with suitable elements that will transform its planar crystal structure, with sp^2 bonds between the carbon atoms, into a three-dimensional structure with sp^3 bonding between them. Theoretical predictions show that hydrogen and fluorine are good candidates to play such a role with an expected band gap of 3.8 eV and 4.2 eV for 100% functionalization, respectively.[2,3]

Successful hydrogenation of monolayer graphene has already been achieved[4,5] but there has been no experimental investigation of fluorinated graphene transistors. In this work we have succeeded in fabricating transistor structures with fluorinated graphene monolayers and studied their transport properties at temperatures from 4.2 to 300 K. Fluorinated graphene flakes were separated by mechanical exfoliation[1] from fluorinated graphite with fluorine contents of 24% and 100%. They are then processed into transistor structures which have shown a strong increase in the resistance in the Dirac region, caused by the opening of a mobility gap in the graphene spectrum.

There are two main ways to produce fluorinated graphite.[6–9] In the first graphite is heated in the presence of F_2 to temperatures in excess of 300 °C so that covalent C—F bonds are formed and modify the carbon hybridization. The layered structure of graphite is then transformed into a three-dimensional arrangement of carbon atoms. In the second, graphite is exposed to a fluorinating agent, XeF_2, and the process is performed at a temperature lower than 120 °C as XeF_2 easily decomposes on the graphite surface into atomic fluorine. Due to its reactivity and diffusion, the fluorination results in a homogenous dispersion of fluorine atoms that become covalently bonded to carbon atoms.[8,10] At low fluorine content (F/C atomic ratio ≤ 0.4), conjugated C=F double bonds in the nonfluorinated parts and covalent C—F bonds in corrugated fluorocarbon regions coexist,[9,11] with the concentration of the covalent bonds increasing with concentration of fluorine.

In this work we use both methods of fluorination of the original graphite material. We first considered fully fluorinated highly oriented pyrolytic graphite $(CF)_n$ as a starting material. The flakes are mechanically exfoliated from the fluorinated graphite onto conventional Si/SiO_2 (275 nm) substrates. The produced flakes are noticeably smaller (~ 1 μm in size) than the flakes fabricated by the same method from nonfluorinated graphite. They contain more than 10 monolayers, it was impossible to produce monolayer fluorinated graphene using this method.

The many-layer exfoliated flakes were first characterized by Raman spectroscopy using excitation light with a wavelength of 532 nm and a spot size of 1.5 μm in diameter. An incident power of ~ 5 mW was used. We ensured that this power does not damage the graphene by performing Raman measurements on a similarly sized pristine graphene flake which shows the common spectra of mechanically exfoliated graphene: the G and 2D bands at 1580 and 2700 cm^{-1}, see Fig. 1(a).

In fully fluorinated graphene, a D peak appears at 1350 cm^{-1} and its intensity is larger than that of the G and 2D peaks, see Fig. 1(b). As the D resonance requires a defect for its activation, its presence is associated with an increased degree of disorder.[12–14] Various defects can contribute to the D peak, such as bond dislocations, missing atoms at the edges of the sample and sp^3-hybridized carbon atoms. Previous studies demonstrated that the intensity of the D peak produced from the edges of a graphene flake is relatively small compared to the G peak.[15] Our experiments consistently show that the D peak of pristine graphene flakes with similar size as fully fluorinated graphene is below the resolution of the measurement, see Fig. 1(a). This suggests that the edges of the fully fluorinated flakes give minimal contribution to the D peak in Fig. 1(b). Furthermore, structural studies[6] of the bulk fully fluorinated graphite material show that the defects are sp^3-bonded carbon atoms and not bond dislocations. Therefore, we expect some contribution to the D peak of fully fluorinated graphene to come from sp^3-bonded carbon atoms.

Several transistor structures have been fabricated from the fully fluorinated flakes using e-beam lithography and deposition of Cr/Au contacts (5 nm of Cr and 50 nm of Au). All the studied devices show very large resistance (more than

 ©2010 The American Physical Society

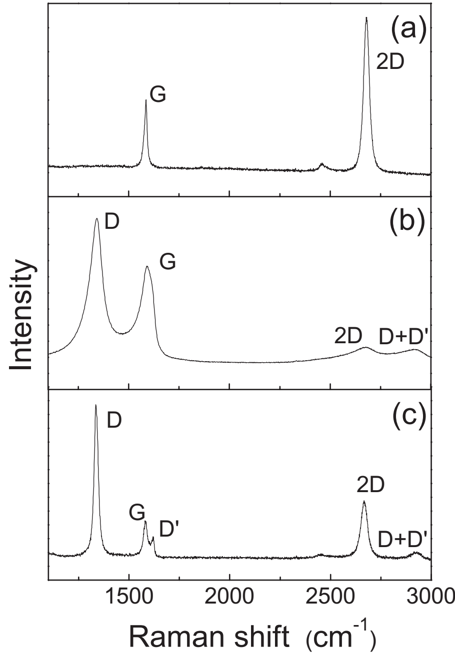

FIG. 1. Raman spectra for (a) pristine graphene, (b) multilayer fully fluorinated graphene, and (c) fluorinated graphene monolayer.

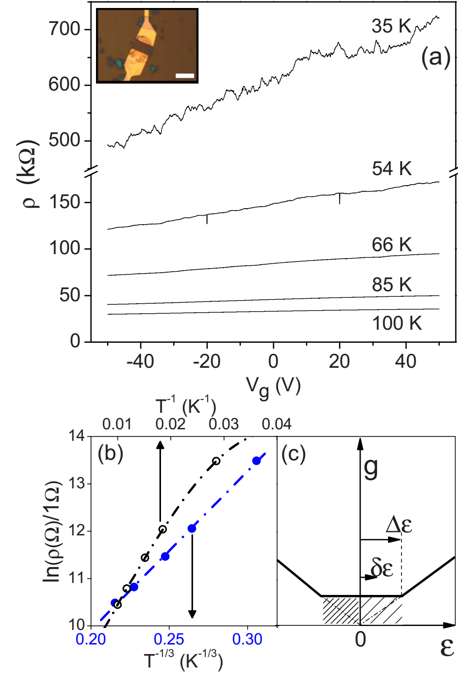

FIG. 2. (Color online) (a) Resistivity as a function of gate voltage for a fully fluorinated device. Inset: optical image of the device (scale bar is 1 μm). (b) Resistivity plotted against T^{-1} and $T^{-1/3}$ at V_g=+50 V. (c) A diagram of the energy dependence of the density of electron states with the Fermi level at zero energy and localized states shown by the shaded area. (Dense shading shows occupied localized states.)

1 GΩ) and no gate-voltage control of the resistance, typical of a wide band-gap semiconductor material. Recent works[16,17] have shown that the I/V characteristics of fully fluorinated graphene are strongly nonlinear with a nearly gate-independent resistance value higher than 1 GΩ, suggesting the presence of a band gap. The purpose of this work is to produce transistor structures with a large on/off ratio of the current. To this end, we reduced the fluorine content by annealing the samples at ~300 °C in a 10% atmosphere of H_2/Ar for 2 h. The resistance is decreased and a partial gate-voltage control is achieved, Fig. 2(a). The annealing, however, has not noticeably changed the Raman spectrum in Fig. 1(b).

Resistance measurements of the fully fluorinated flakes after annealing show a strong temperature dependence, Fig. 2(a). To examine the presence of the energy gap, we analyzed $\rho(T)$ at the highest gate voltage V_g=50 V (which is still far from the Dirac point) by an exponential law describing thermal activation of carriers across the energy gap $\Delta\epsilon$: $\rho=\rho_0 \exp(\Delta\epsilon/2k_BT)$, Fig. 2(b). The resulting value of $\Delta\epsilon$ found at high temperatures is only ~25 meV, which is significantly smaller than the expected energy gap for fully fluorinated graphene. It is also seen that the slope of ln $\rho(1/T)$ dependence decreases with decreasing T, which is a signature of hopping conduction via localized states.[18] The fact that in the whole range of studied temperatures electron transport is not due to thermal activation across the gap but due to hopping, has been confirmed by reanalyzing the temperature dependence in terms of two-dimensional hopping: $\rho(T)=\rho_0 \exp(T_0/T)^{1/3}$, where $k_BT_0=13.6/a^2g(\mu)$, g is the density of localized states at the Fermi level μ and a is the localization length.[18] The results are found to be in good agreement with this expression, Fig. 2(b), with the value of T_0=20 000 K. This confirms that the previously found activation energy of 25 meV is not the activation energy $\Delta\epsilon$ that separates the localized states from extended states at the mobility edge but is an activation energy $\delta\epsilon$ of hopping between localized states within the mobility gap, Fig. 2(c). Although not measured, the value of $\Delta\epsilon$ in these samples seems to be larger than that in hydrogenated graphene, as the obtained value of T_0 is ~100 times larger than in Ref. 5, indicating a smaller density of localized states and smaller localization length.

To achieve good V_g control of fluorinated graphene transistors, one needs to fabricate monolayer flakes. To do this, we have used the second method of fluorination by gaseous XeF_2. The mixture of natural graphite and XeF_2 was prepared in a glove box in an Ar atmosphere. The reactor was then kept at 120 °C for 48 h, which gave a fluorine content of 24% as measured by mass uptake. Mechanical exfoliation of the partially fluorinated graphite is carried out under ambient conditions. Flakes are located using an optical microscope and monolayer flakes with an optical contrast of ~5–7 % in green light were selected for processing into transistor structures. (We noticed that the contrast of fluorinated monolayers is ~2% lower than that of pristine graphene on Si/SiO_2 (275 nm) substrates.) The flakes were confirmed to be monolayer by Raman spectroscopy. The 2D peak which is well fitted by a single Lorentzian function, and has a full width at half maximum in the region of 20–30 cm^{-1} is typical for pristine monolayer graphene.[12]

The Raman spectrum of partially fluorinated monolayer graphene, Fig. 1(c), shows much narrower D, G, and 2D

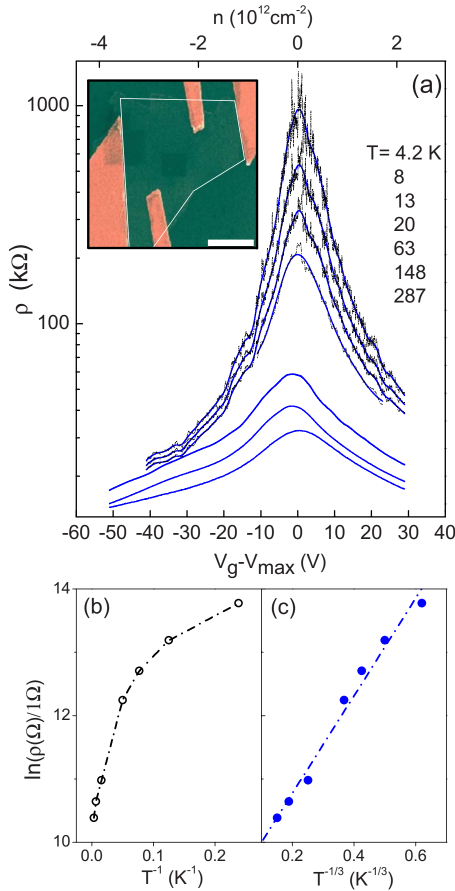

FIG. 3. (Color online) (a) Resistivity of fluorinated monolayer graphene as a function of gate voltage. Inset: false color scanning electron microscopy image of the monolayer device (scale bar is 1 μm). Resistivity in the Dirac region plotted as a function of (b) T^{-1} and (c) $T^{-1/3}$.

peaks compared with thicker layers made from fully fluorinated graphite, Fig. 1(b). This made it possible to detect additional features in the Raman spectrum that also arise in hydrogenated graphene:[5] the D′ peak at ≈1620 cm^{-1}, which also requires a defect for its activation, and a combination mode (D+D′) at ≈2950 cm^{-1}. It is interesting to note that in our fluorinated graphene the ratio of the integrated intensities I_D/I_G=3.8, which is larger than that found in partially (on one side) hydrogenated sample, and is comparable to that in the samples hydrogenated on both sides.[5] This can be the result of the fact that in the monolayer flakes fabricated by exfoliation from fluorinated (intercalated) graphite the probability of fluorination is equal for both sides of the plane.

In total, four monolayer flakes were processed into four-terminal transistor devices. Figure 3(a) shows the resistance as a function of gate voltage measured for a range of temperatures. (Comparisons of two- and four-probe measurements have shown that the contact resistance is negligible compared with the sample resistance, which indicates a good Ohmic contact between the Cr and fluorinated graphene.) Due to the small size of the samples, ~4 μm^2 in area, the resistance shows strong mesoscopic fluctuations,[19] and thus the $R(V_g)$ dependences were smoothed for the subsequent analysis using a moving average filter.

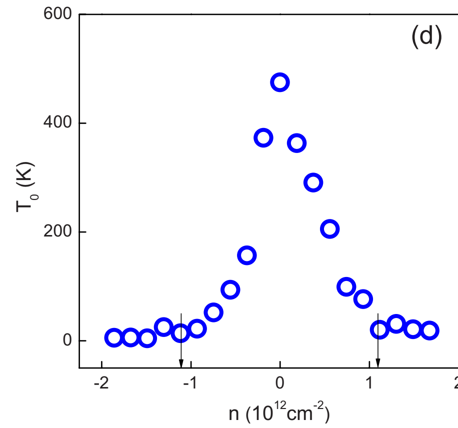

FIG. 4. (Color online) (a) The value of the hopping parameter T_0 as a function of the carrier density. Arrows indicate the concentration at which T_0 approaches zero and the conduction becomes metallic.

The curves in Fig. 3(a) have been offset along the V_g axis to account for doping, which is detected as a shift of the maximum resistance (the Dirac point) from V_g=0. The partially fluorinated samples were found to be doped to V_g=+10 V (n=0.74×10^{12} cm^{-2}). This level of doping is similar to that seen in conventional (pristine) graphene devices, which we attribute to doping by atmospheric water. Unlike pristine graphene devices with very weak temperature dependence of the resistance, in the range of V_g=±20 V around the Dirac point the resistivity of fluorinated samples is seen to grow by 2 orders of magnitude as T decreases from 300 to 4.2 K. Outside this region the temperature dependence remains weak with the mobility of carriers ~150 cm^2 V^{-1} s^{-1}.

Analysis of the temperature dependence of the resistance in terms of the activation law, $\rho=\rho_0 \exp(\Delta\epsilon/2k_BT)$, shows that it is not applicable for the whole temperature range and at high temperatures gives an activation energy of ~7 meV at the neutrality point. Similarly to the fully fluorinated layers, the resistivity $\rho(T)$ is fitted well by variable range hopping, $\rho(T)=\rho_0 \exp(T_0/T)^{1/3}$, Fig. 3(c). Figure 4 shows the hopping parameter T_0 as a function of carrier concentration. The value of T_0 approaches zero at a carrier concentration of ±1.2×10^{12} cm^{-2}. This value gives the concentration of the localized electron states in the energy range from ϵ=0 to the mobility edge. The mobility edge occurs at $V_g\simeq\pm20$ V and indicates the transition from hopping to metallic conduction, Fig. 2(c).

In order to relate the obtained concentration of the localized states to the energy gap $\Delta\epsilon$, one needs to know the exact energy dependence of the density of states in the gap. For estimations, we will use the linear relation for the density of extended states above the mobility edge, $g(\epsilon)=2\varepsilon/\pi\hbar^2v^2$ (v=10^6 m s^{-1} is the Fermi velocity) and a constant value for the density of localized states below the mobility edge, Fig. 2(c). This gives an estimation $\Delta\epsilon$~60 meV and twice this value for the full mobility gap. In this approximation the density of the localized states in the gap is estimated as 10^{36} J^{-1} m^{-2}. Using the obtained value of the hopping parameter T_0~500 K in the Dirac point, one can then estimate the localization length at ϵ=0 as a~40 nm.

The presence of localized states in the electroneutrality region is clearly the result of disorder due to the random positions of F atoms on graphene in the partial fluorination. The current experiment does not allow us to establish whether these states exist in the band gap produced by fluorination or are simply the result of a "smearing" of the linear density of states of graphene [as sketched in Fig. 2(c)]. Taking into account the relatively small value of the parameter T_0 and large localization radius a, it seems that the latter case is most probable and there is no large band gap created in the spectrum. For future applications, however, it is only an increase in the resistance in the electroneutrality region which matters and this is achieved in both scenarios of creation of the mobility gap. Our results show that in order to achieve large resistances in graphene transistors at room temperature, future efforts should be aimed at decreasing the density of localized states in the mobility gap and decreasing the localization length, which can be done by partial fluorination with the fluorine content in the range between our studied values of 24% and 100%.

In conclusion, the possibility of fabricating a transistor structure using fluorinated monolayer graphene has been demonstrated. Fluorination has been shown to cause a significant increase in the resistance in the electroneutrality region, which is a consequence of the creation of the mobility gap in the electron spectrum where electron transport is through localized states.

We are grateful to A. V. Shytov for useful discussions and A. A. Kozikov for help with measurements, and to EPSRC for funding.

[1] A. K. Geim and K. S. Novoselov, Nature Mater. **6**, 183 (2007).
[2] J. O. Sofo, A. S. Chaudhari, and G. D. Barber, Phys. Rev. B **75**, 153401 (2007).
[3] D. W. Boukhvalov and M. I. Katsnelson, J. Phys.: Condens. Matter **21**, 344205 (2009).
[4] S. Ryu *et al.*, Nano Lett. **8**, 4597 (2008).
[5] D. C. Elias *et al.*, Science **323**, 610 (2009).
[6] T. Nakajima, in *Fluorine-Carbon and Fluoride-Carbon Materials*, edited by T. Nakajima (Marcel Dekker, New York, 1995), Chap. 1.
[7] K. Touhara and K. Okino, Carbon **38**, 241 (2000).
[8] W. Zhang *et al.*, J. Fluorine Chem. **131**, 676 (2010).
[9] Y. Sato, K. Itoh, R. Hagiwara, T. Fukunaga, and Y. Ito, Carbon **42**, 3243 (2004).
[10] W. Zhang *et al.*, Carbon **46**, 1010 (2008).
[11] J. Giraudet *et al.*, J. Phys. Chem. B **111**, 14143 (2007).
[12] A. C. Ferrari *et al.*, Phys. Rev. Lett. **97**, 187401 (2006).
[13] A. C. Ferrari and J. Robertson, Phys. Rev. B **61**, 14095 (2000).
[14] A. C. Ferrari, Solid State Commun. **143**, 47 (2007).
[15] C. Casiraghi *et al.*, Nano Lett. **9**, 1433 (2009).
[16] S. Cheng, K. Zou, F. Okino, H. Gutierrez, A. Gupta, N. Shen, P. Eklund, J. Sofo, and J. Zhu, Phys. Rev. B **81**, 205435 (2010).
[17] R. Nair, W. Ren, R. Jalil, I. Riaz, V. Kravets, L. Britnell, P. Blake, F. Schedin, A. Mayorov, S. Yuan, M. Katsnelson, H. Cheng, W. Strupinski, L. Bulusheva, A. Okotrub, K. Novoselov, A. Geim, I. Grigorieva, and A. Grigorenko, arXiv:1006.3016 (unpublished).
[18] B. I. Shklovskii and A. L. Efros, *Electronic Properties of Doped Semiconductors*, Springer Series in Solid State Sciences Vol. 45 (Springer, Berlin, 1984).
[19] K. Kechedzhi, D. W. Horsell, F. V. Tikhonenko, A. K. Savchenko, R. V. Gorbachev, I. V. Lerner, and V. I. Fal'ko, Phys. Rev. Lett. **102**, 066801 (2009).